VEHICLE COMPARTMENTS ENVIRONMENTAL CONTROL SYSTEM USING SOLAR POWERED THERMOELECTRIC
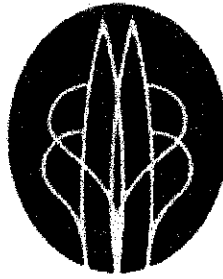
UNIVERSITI
TEKNOLOGI
PETRONAS

By

OMAR BIN ABDUL AZIZ

FINAL PROJECT REPORT

Submitted to the Electrical & Electronics Engineering Programme
in Partial Fulfillment of the Requirements
for the Degree
Bachelor of Engineering (Hons)
(Electrical & Electronics Engineering)

Universiti Teknologi Petronas
Bandar Seri Iskandar
31750 Tronoh
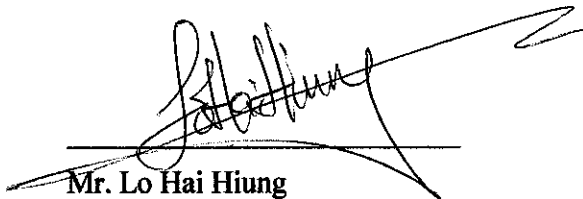Perak Darul Ridzuan

ii

CERTIFICATION OF APPROVAL

VEHICLE COMPARTMENTS ENVIRONMENTAL CONTROL SYSTEM USING SOLAR POWERED THERMOELECTRIC

by

Omar Bin Abdul Aziz

A project dissertation submitted to the
Electrical & Electronics Engineering Programme
Universiti Teknologi PETRONAS
in partial fulfilment of the requirement for the
Bachelor of Engineering (Hons)
(Electrical & Electronics Engineering)

Approved:

_____
Mr. Lo Hai Hiung
Project Supervisor

UNIVERSITI TEKNOLOGI PETRONAS

TRONOH, PERAK

December 2005

CERTIFICATION OF ORIGINALITY

This is to certify that I am responsible for the work submitted in this project, that the original work is my own except as specified in the references and acknowledgements, and that the original work contained herein have not been undertaken or done by unspecified sources or persons.

Omar Bin Abdul Aziz

ABSTRACT

This project investigate the feasibility of using solar powered thermoelectric-technology device, to act as a temperature regulator system for vehicle cabin. The temperature regulator system's intended function is to control temperature of vehicle cabin under parked, sun-exposed condition, in order to mitigate the problem of overheated vehicle compartment. The studies which depend largely on researches, is to construct a working prototype to aid in the analysis performed. A design plan on suitable power supply for the temperature regulator system will be introduced and evaluated for practical application on real vehicle. Further improvement works are recommended to enhance the performance and practicality of the design introduced.

ACKNOWLEDGEMENTS

In the name of Allah, the Most Gracious, the Most Merciful. Praise to Him the Almighty, that in His will and given strength, had I managed to complete this final year project.

A lot has transpired throughout the process of completing this project, and I am indebt to many who had made this course an illuminating and enriching venture. My deepest gratitude goes to my supervisor, Mr. Lo Hai Hiung, who's continuous support, supervision and invaluable suggestions had played a significant part in the completion of the project.

My sincere and heartfelt thanks to Ir. Shiraz, Mr. Zaihar and Dr. Nazer Ahmad for their enlightening ideas and time spent in sharing their insightful understanding and profound knowledge, with regards to subject matters relevant to this project. I would like to express my full appreciation towards Electrical & Electronics laboratory assistances, namely Mr. Azhar and Ms. Siti Hawa for their assistant and guidance.

I am grateful to all the lecturers and UTP staffs, who were so helpful and their never-ending supports 'with a smile' had made the project's completion a memorable and an informative one. Kudos goes to my family who had given the moral support which had truly been a great inspiration. Last but not least to my fellow colleagues, who have directly or indirectly lent a helping here and there.

Thank you one, thank you all.

TABLE OF CONTENTS

LIST OF TABLES

LIST OF FIGURES

LIST OF ABBREVIATIONS

Symbol	Meaning	Unit
UTP	Universiti Teknologi Petronas	
DC	Direct Current	
BTU	British Thermal Unit	
PV	Photovoltaic	
PWM	Pulse Width Modulator	
Ah	Ampere-hour	
Q	cooling load	W
U	overall heat transfer coefficient	$W/(m^2K)$
A	Area	m^2
CLTD	corrected Cooling Load Temperature Difference	K
GLF	Glass Load Factor	K

CHAPTER 1

INTRODUCTION

1.1 Background Study

In equatorial countries, where the weather is generally hot and humid throughout the year, vehicle owners have to live with overheated vehicle compartments especially when the vehicle have been parked under the sun. A car parked on a hot day can quickly become a virtual oven. Temperature inside a stationary car can rapidly increase to double that on the outside temperature, within six to ten minutes depending on the weather conditions.

Temperatures at this level do not only damage car interior and items left in the car, but also poses a threat to human lives. Children, elders and pets left in parked cars, though it's just for a couple of minutes, are at risk of heat stroke which can lead to death. High temperatures coupled with the presence of high humidity further increases the likelihood of heat stroke. In addition, the sudden change of temperature experienced when entering a car parked under the sun, may cause headaches, sweating, dizziness and discomfort[1].

While the choice of a cooling technology depends heavily on the unique requirements of any given application, this project presents a study on the feasibility of using thermoelectric technology device to regulate vehicle cabin temperature under sun-exposed parked condition.

1.2 Problem Statement

This project was embarked to study the feasibility of using thermoelectric module to regulate the temperature inside a vehicle compartments. One of the major concerns identified in using thermoelectric module, or popularly known as the Peltier module is that it can draw a substantial amount of current [2]. For this reason, a sufficient

power supply that would cater the power requirement of thermoelectric module operation is in need.

This is when solar power *enter the picture* of the project, as a possible power source to be exploited and employed to power up the Peltier module. With virtually limitless energy, and no recharging required, the sun is a great potential of power source. Today's more efficient, less expensive solar cells provide a practical mean of converting the sun's power into electricity.

Nevertheless, as clouds often obscure the sun, it's tough to design a system that can reliably provide power sufficient to the need of the load [3]. Thus, a careful approach in harnessing the solar power is a must to optimise power source that can be generated, and subsequently supplied to the Peltier module.

1.3   Objectives and Scope of Study

1.3.1   Objectives

1. To calculate the power source that may be required by the thermoelectric based temperature regulator system for a typical road vehicle.
2. To come up with a power supply system, making use of solar power source to power the thermoelectric based temperature regulator system.
3. To design and built a prototype of the power supply system to demonstrate its workability as well as efficiency .

1.3.2   Scope of Study

To ensure the success completion of the project, the scope of study of the project will be focusing on:

1. The principle, operation and limitation of thermoelectric-technology device

2. Solar panel operating principle

3. Battery storage operating principle

4. Thermal load theory and cooling load estimation

5. Circuit theory and circuitry design

6. Cooling system analysis for practical application

CHAPTER 2

LITERATURE REVIEW AND THEORY

2.1 Thermoelectric Cooling and Power Generation

2.1.1 Thermoelectric cooling and Peltier module

The basic concept behind thermoelectric cooling technology is the Peltier effect; a phenomenon first discovered in the early 19th century. The Peltier effect occurs whenever electrical current flows through two dissimilar conductors; depending on the direction of current flow, the junction of the two conductors will either absorb or release heat.[2]
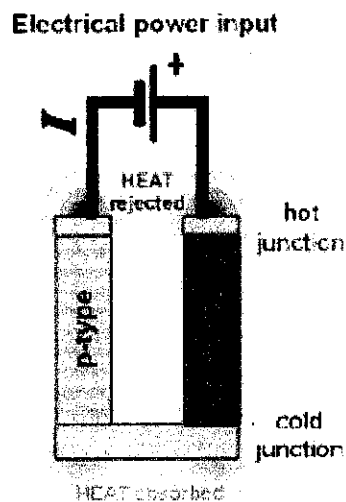
Figure 1   Heat is pumped from the cold to hot junction[4]

Semiconductors, usually Bismuth Telluride, are the material of choice for producing the Peltier effect, as they can be optimized more easily for pumping heat, and because designers can control the type of charge carrier employed within the conductor. If an electric current is applied to the thermocouple as

shown above in **Figure 1**, heat is pumped from the cold junction to the hot junction. The cold junction will rapidly drop below ambient temperature provided heat is removed from the hot side. The temperature gradient will vary according to the magnitude of current applied.

In order to give a thermoelectric device greater heat-pumping capacity, multiple pellets are used together. By arranging N and P-type pellets in a 'couple' and forming a junction between them with a plated copper tab, it is possible to configure a series circuit which can keep all of the heat moving in the same direction. As shown in **Figure 2**, with the free (bottom) end of the P-type pellet connected to the positive voltage potential and the free (bottom) end of the N-type pellet similarly connected to the negative side of the voltage.
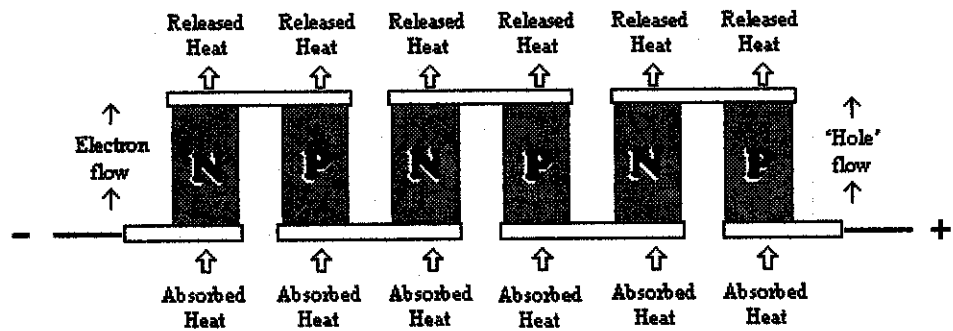
Figure 2   Multi-couple configuration increases heat pumping capacity[3]

The positive charge carriers, holes, in the P material are repelled by the positive voltage potential and attracted by the negative pole. The negative charge carriers, electrons, in the N material are likewise repelled by the negative potential and attracted by the positive pole of the voltage supply. In the copper tabs and wiring, electrons are the charge carriers; when these electrons reach the P material, they simply flow through the 'holes' within the crystalline structure of the P-type pellet. As the charge carriers inherent in the material structure dictate the direction of heat flow, the electrons flow continuously from the negative pole of the voltage supply, through the N pellet, through the copper tab junction, through the P pellet, and back to the positive pole of the supply. As two different types of semiconductor material

16

are used, the charge carriers and heat are all flowing in the same direction through the pellets[2].

A typical Peltier module as in **Figure 3**, consists of N and P semiconductors mounted successively, which form p-n- and n-p-junctions. With the special properties of the thermoelectric 'couple' teamed in rectangular arrays, it is possible to create practical thermoelectric modules. These devices can not only pump appreciable amounts of heat, but with their series electrical connection, are suitable for commonly-available DC power supplies.

cold side

semiconductor
of p-type
semiconductor
of n-type isolator   hot
(ceramics)   side

conductor
(copper)
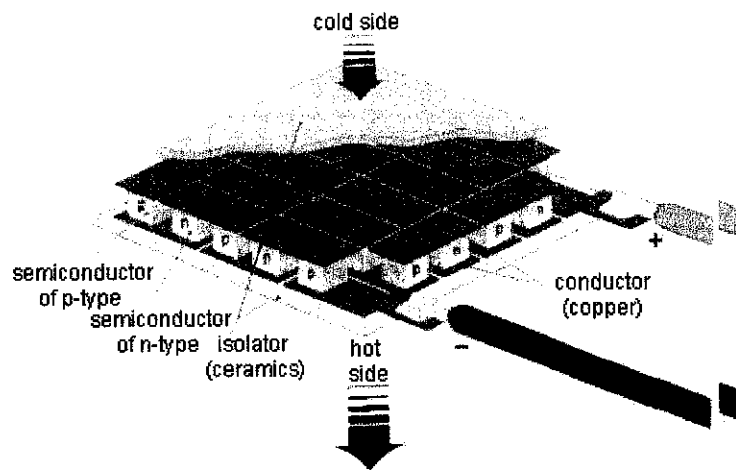
Figure 3: Typical Peltier module[5]

The flow of heat with the charge carriers in a Peltier module, is very similar to the way that compressed refrigerant transfers heat in a mechanical system. The circulating fluids in the compressor system carry heat from the thermal load to the evaporator where the heat can be dissipated. With thermoelectric technology, on the other hand, the circulating direct current carries heat from the thermal load to some type of heat sink, illustrated in **Figure 4**, which can effectively discharge the heat[6].
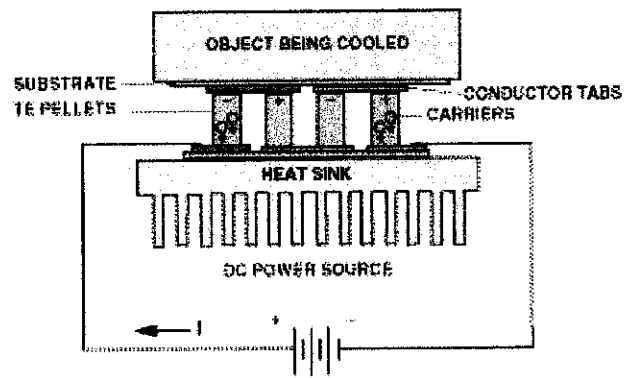
Figure 2

Figure 4   Typical Peltier module assembly[6]

Each individual thermoelectric system design will have a unique capacity for pumping heat in Watts or British Thermal Unit(BTU)/hour and this will be influenced by many factors. The most important variables are ambient temperature, physical & electrical characteristics of the thermoelectric module employed, and efficiency of the heat dissipation system. Typical thermoelectric applications will pump heat loads ranging from several milliwatts to hundreds of watts.

2.1.2   Thermoelectric power generation

Whenever an electrical conductor is strung between two different temperatures, the conductor is capable of transferring thermal energy from the warmer side to the colder one. Furthermore, the physical process of transferring that heat, also tends to move electrical charge carriers within the conductor in the same direction as the heat. Conceivably then, this charge carrier movement can be used to generate electrical current[6].

If two dissimilar conductors are employed,. with differing capacities for moving charge carriers in response to thermal flow, the current level in one conductor will overcome the potential for thermally-generated current flow in the other conductor. The net effect is a continuous current level which is equal to the generated current capacity of the primary conductor for the given temperature difference, minus the generated current capacity of the second conductor. The existence of this net current flow, indicates that a voltage is

18

created through the movement of heat and a direct measurement of this voltage level can be obtained by breaking the circuit and measuring across the opened terminals with a voltmeter. The ability of two dissimilar conductors to produce a voltage when a temperature difference is applied, is called the Seebeck effect. The voltage which results is referred to as Seebeck voltage[6].
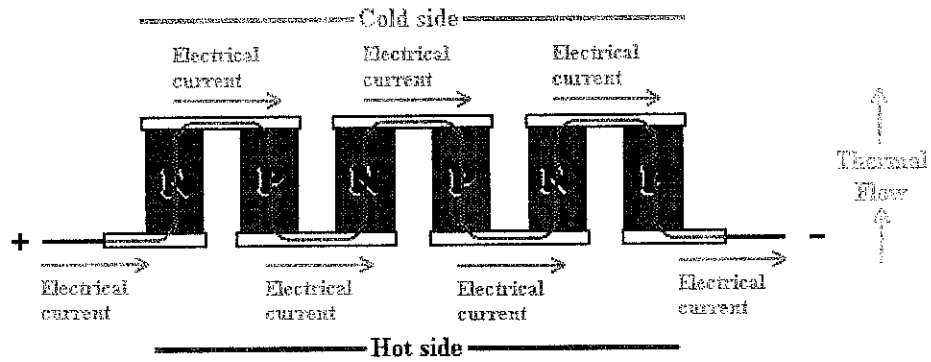
Figure 5 **Electrical current generated by thermoelectric temperature differences[6]**

2.2 Solar Panel

Solar panels work on the principle of the photovoltaic (PV) effect. The PV effect is the conversion of sunlight into electricity. This occurs when the PV cell is struck by photons from the sunlight, thus 'freeing' silicon electrons to travel from the PV cell, through electronic circuitry, to a load as in **Figure 6**. Then they return to the PV cell, where the silicon recaptures the electron and the process is repeated. Solar panel produce voltage when illuminated, dependent upon the light intensity and the load but independent of surface area.

19
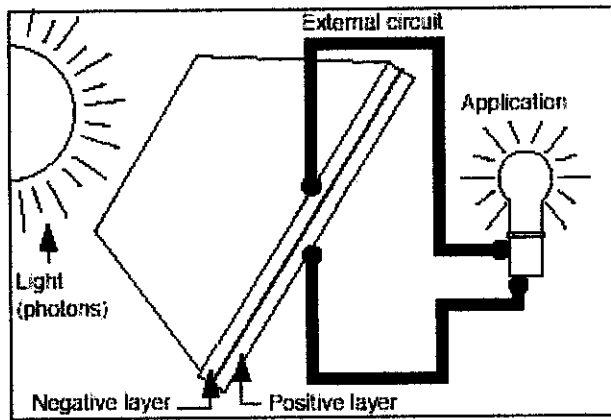
Figure 6   Principle of operation[7]

The important characteristic which makes this type of solar panel suitable for supplying electrical power is that the voltage builds up quickly to a reliable plateau at very low light levels, about 8% of peak intensity. This means that voltages suitable for battery charging are reached even on a dull day. Current, however, is directly proportional to both light intensity and surface area[7].
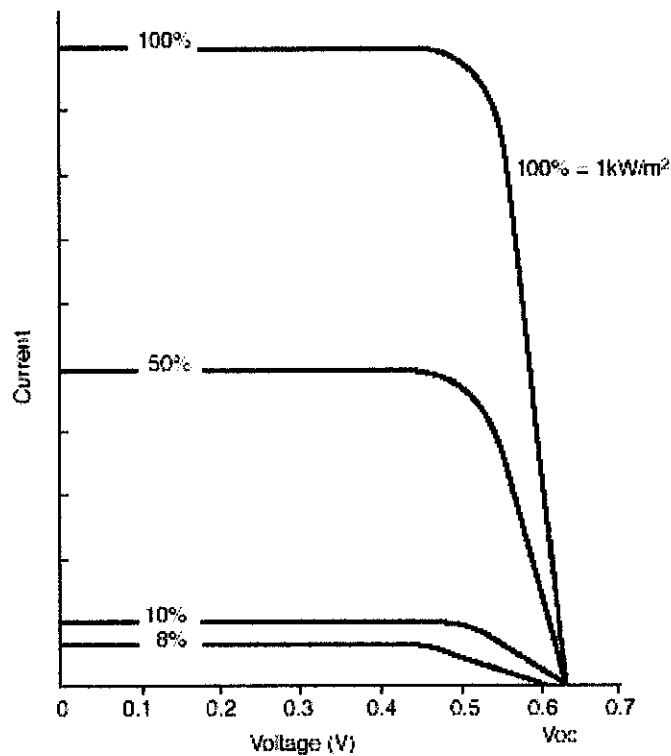
Figure 7   I-V characteristics at reducing light intensities[7]

A solar panel active area which is the frontal area that generates electrical power is a critical design consideration in using any photovoltaic product. If this area is covered by a mounting bezel, power may be reduced and the product may cease to function. For optimal performance, the active area must never be shaded.

PV cell consists of two or more thin layers of semi-conducting material, most commonly silicon. When the silicon is exposed to light, electrical charges are generated and this can be conducted away by metal contacts as direct current (DC) [8]. The electrical output from a single cell is small, so multiple cells are connected together and encapsulated, usually behind glass to form a solar panel. There are many types of solar cells which differ from each other based on how the silicones are made into cells. The most common four types of PV cells are[9] :

2.2.1 Monocrystalline silicon cell

Made using cells saw-cut from a single cylindrical crystal of silicon, this is the most efficient of the photovoltaic (PV) technologies. The principle advantage of monocrystalline cells are their high efficiencies, typically around 15%, although the manufacturing process required to produce monocrystalline silicon is complicated, resulting in slightly higher costs than other technologies.
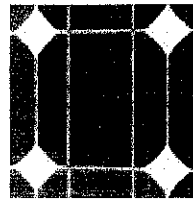
Figure 8   Monocrystalline silicon cell

2.2.2 Multicrystalline silicon cell

Multicrystalline silicon cell is made from cells cut from an ingot of melted and recrystallised silicon. In the manufacturing process, molten silicon is cast into ingots of polycrystalline silicon, these ingots are then saw-cut into very thin wafers and assembled into complete cells. Multicrystalline cells are cheaper to produce than monocrystalline ones, due to the simpler

21

manufacturing process. However, they tend to be slightly less efficient, with average efficiencies of around 12%, creating a granular texture.
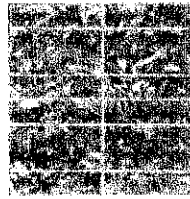
Figure 9   Multicrystalline silicon cell

2.2.3   Thick-film silicon cell

This type of silicon cell is another multicrystalline technology where the silicon is deposited in a continuous process onto a base material giving a fine grained, sparkling appearance. Like all crystalline PV, this is encapsulated in a transparent insulating polymer with a tempered glass cover and usually bound into a strong aluminium frame.
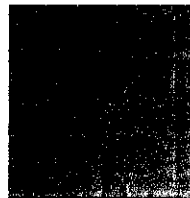
Figure 10   Thick-film silicon cell

2.2.4   Amorphous silicon cell

Amorphous silicon cells are composed of silicon atoms in a thin homogenous layer rather than a crystal structure. Amorphous silicon absorbs light more effectively than crystalline silicon, so the cells can be thinner. For this reason, amorphous silicon is also known as a "thin film" PV technology. Amorphous silicon can be deposited on a wide range of substrates, both rigid and flexible, which makes it ideal for curved surfaces and "fold-away" modules. Amorphous cells are, however, less efficient than crystalline based cells, with typical efficiencies of around 6%, but they are easier and therefore cheaper to

produce. Their low cost makes them ideally suited for many applications where high efficiency is not required and low cost is important.
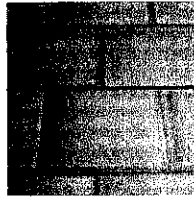
Figure 11   Amorphous Silicon Cell

CHAPTER 3

METHODOLOGY

3.1 Procedures

3.1.1 Research

Researches have been carried out on a broad area of studies that fall under area of discussion, namely pertaining to thermoelectric cooling, solar panel, battery utilisation and electrical circuitry for battery charging. For thermoelectric cooling, the author had acquire findings regarding its operating principle, performance, as well currently used applications of the technology. Researches on solar panel efficiency and limitation in converting sun light to electricity is also explored to make deduction of its feasibility to be a practical power source for practical vehicle cabin's temperature regulator system.

Studies on batteries has its way in the project when it was decided to make use of batteries to complement the limitations of solar panel sourcing. Studies were mainly focusing on the charging and discharging of batteries. Therefore, investigation on the most suitable battery charger circuitry to suit the project was also explored.

3.1.2 Experiments and data gathering

One of the first experiments conducted was to measure the temperatures of vehicle cabin, between 10 am until 2pm, for a period of six days. The temperature values obtained were crucial in calculating heat load, hence the cooling power that is required for the project. Tests were also conducted on

the acquired solar panel to observe and examine the influence of weather on output power generated.

After understanding the concept of thermoelectric and thermal cooling, several experiments were conducted on the Peltier module. The experiments involved the use of Peltier modules, whereby the author had analysed the heat-influential effect of supplying power to the modules, as well as power generation capability of the Peltier module. This is for the purpose of knowing precautions to be taken into account when supplying power to the Peltier modules in the prototype and evaluating the possible use of Peltier module for power generation. Another important experiment conducted was to test the operation of Peltier modules, with heatsink for better heat dissipation of Peltier module's hot side. Several heatsinks were tested for this purpose.

3.1.3 Constructing a prototype

The prototype was constructed part by part accordingly with the acquirement of the components required. The author have also performed circuitry simulations by using PSpice Version 9.2.3 application tools to aid in the design. **Figure 12** below shows the project's flow chart in constructing the prototype:
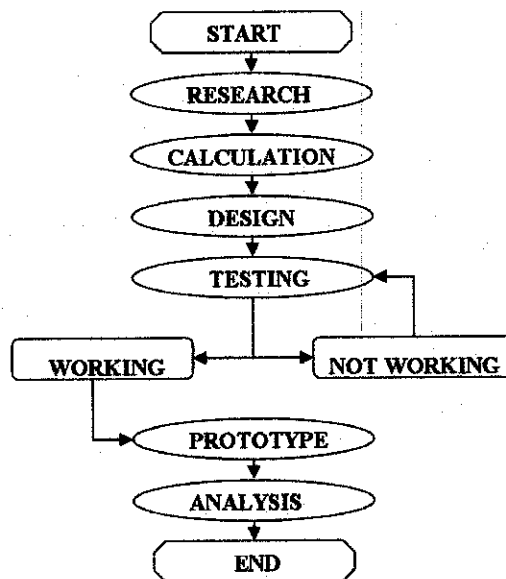
Figure 12   Prototype's construction flowchart

3.2 Tools Required

the hardware required for the construction of the prototype are listed as below in **Table 1.**

Table 1   List of components and tools

Tools/ Components	Amount
Solar panel (RS 194-133)	2
Sealed acid lead battery	1
Breadboard	1
Veraboard	1
50 kΩ resistor	2
10 kΩ resistor	2
5 kΩ resistor	8
1 kΩ resistor	2
300Ω resistor	2
0.01μF capacitor	2
0.001μF capacitor	2
0.47μF capacitor	2
1N4007 diode	2
47μH	2
PN2222A PNP transistor	2
C9012 PNP transistor	2
LM3524D PWM	2

Software used:

1. PSpice Version 9.2.3

CHAPTER 4

RESULTS AND DISCUSSIONS

4.1 Results

4.1.1 Cooling load calculation

Shown in **Table 2** are the temperature measurements of car cabin for six days, which has been parked in UTP student's residential parking area. **Figure 13** shows the data in graphical form. As early as 10 a.m. in the morning, the temperature of car cabin can exceeds 40°C. From the pattern of graphs plotted, it can be said generally that car cabin's temperature is at its highest peak at 12 p.m. in the afternoon. The highest recorded temperature was 64°C.

Table 2   Temperature measurements inside a car cabin (10 a.m.→ 2 p.m.)

Date/Time	10 A.M	11 A.M	12 P.M	1 P.M	2 P.M
14-Mar-05	42°C	42°C	64°C	56°C	45°C
15-Mar-05	40°C	41°C	59°C	59°C	58°C
16-Mar-05	41°C	41°C	62°C	57°C	53°C
17-Mar-05	42°C	42°C	58°C	55°C	45°C
18-Mar-05			56°C	57°C	61 °C
20-Mar-05	36°C	40°C	50°C	61°C	60°C
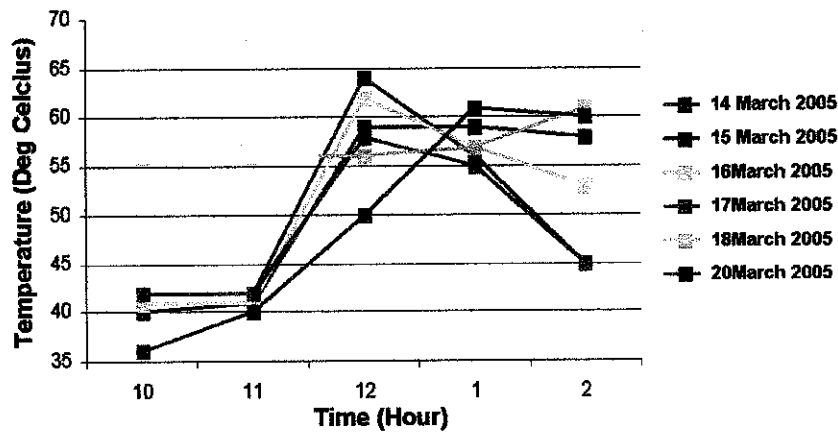
Figure 13 Temperature measurements inside a car cabin (10 a.m.→ 2 p.m.)

Since the normal human body temperature is about 37°C, it was predetermined that the temperature regulator system should regulate vehicle cabin's temperature to be below than 37°C. With the highest temperature recorded being 64°C, ΔT = (64-37) °C = 27°C. The maximum cooling load required for the thermoelectric-based system was calculated using the equation below:

ΔT = [1 - (Heat Load/Max Cooling Power)] x (Max Temp Difference)[10]

27°C = [1 - (Heat Load/Max Cooling Power)] x (Max Temp Difference)

27°C = [1 - (1209.69W /Max Cooling Power)] x (68°C)

Max. cooling power = **2006.32 W**

The Maximum Temperature Difference is the maximum temperature difference that can be achieved between the cold side and the hot side of the Peltier module, which is typically 68°C. Please refer to **APPENDIX A** for calculations of the heat loads.

4.1.2 Solar panel analysis

For this project, two RS 194-133 multicrystalline solar panel were acquired. The output voltage and current ratings of these solar panels are 7.5V and 135mA respectively. **Table 3** shows recorded output measurement from experimenting with the solar panels.

Table 3   Recorded output measurements of RS194-133 solar panels

	Voltage(V)	Current(mA)
Maximum output readings	9.4	180
Minimum output readings (time later than 7.30 a.m)	7.7	40
Maximum output readings (time at 7.30 a.m)	7.5	130

4.1.3   Peltier module and heat sink analysis

For this project, TES1-12704 Peltier module model by Hebeiltd Co. Ltd. were purchased to test and analyse the cooling as well as power generation capability of thermoelectric-based device. For this purpose, the set-up as shown in **Figure 14** was prepared.
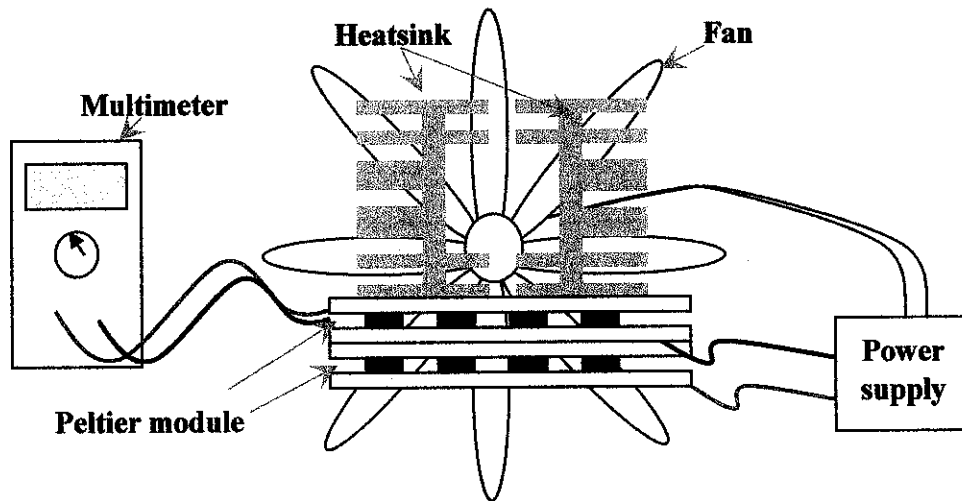
Figure 14   Experiment's set-up for heatsink & Peltier module analysis

Power was supplied to the Peltier module at the bottom (Peltier module1), while the Peltier module above it (Peltier module 2) was connected to a Multimeter. The hot side of Peltier module 1 was allowed to be in contact with Peltier module 2. With this set-up, Peltier module 1 acted as the cooling mechanism, while Peltier module 2 would harness the dissipated heat from the hot side to generate electricity. The heat sink provided better heat dissipation at the upper side, hence allowing a temperature difference between the upper and

29

lower side of Peltier module 2. **Table 4** below shows the resulting measurements.

Table 4   Peltier module analysis measurements

	Voltage readings (V)		Current readings (A)	
	V_{in} Max	V_{out} Max	I_{in} Max	I_{out} Max
Recorded measurement for Peltier module 1	7.3	-	1.03	-
Recorded measurement for Peltier module 2	-	0.5	-	0.04

It was noted that if power is supplied to Peltier module 1 exceeds the recorded maximum voltage and current input, the cold side of the Peltier module cannot sustain its chillness and would become hot due to heat conduction from the hot side. To increase the Peltier module's performance, the experiment was repeated using thermalpaste and larger heatsink. Larger heatsink would provide more area in contact with the thermal load. Thermalpaste is a grease-like product that contains silicon material and is filled with thermally conductive and electrically insulating ceramics. Applying it between the Peltier module and the heat sink would improve heat transfer for better heat dissipation through the heat sink. For this purpose, set-up shown in **Figure 15** was prepared. **Table 5** shows the resulting measurements for the new set-up.
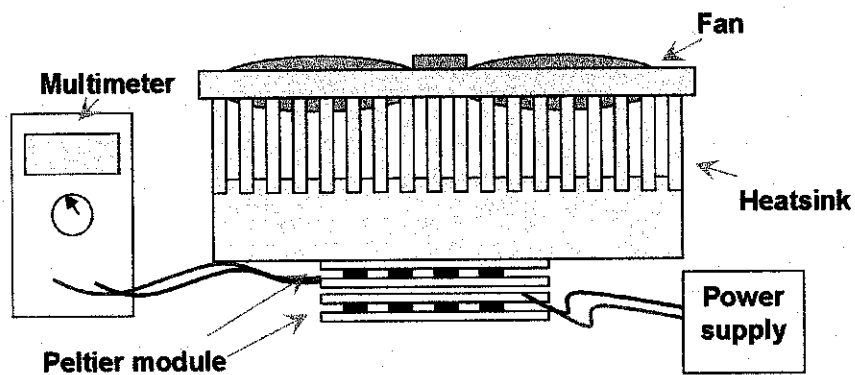
Figure 15   Peltier module analysis with improved heatsink and thermalpaste

Table 5   Peltier module analysis measurements

	Voltage readings (V)		Current readings (A)	
	V_{in} Max	V_{out} Max	I_{in} Max	I_{out} Max
Recorded measurement for Peltier module 1	8.4	-	1.37	-
Recorded measurement for Peltier module 2	-	0.7	-	0.06

4.1.4   Power supply system design

The power supply system design would be based on the output rating of the RS194-133 solar panel. Solar panel's output current strongly varies with light intensity variation of the sun, thus is not a suitable choice of direct power supply to the Peltier module. Therefore, a battery which act as an intermediate energy-storage device, will be used to power up the Peltier module, to ensure an always-ready source of power. The solar panel in-turn will act as a battery charger. For the design, the battery to be used is an *ASANO* 6V- 4Ah rechargeable lead-acid battery.

Because the output voltage of RS194-133 solar panel is higher than that of the battery, it is possible to use it as a battery charger. However, this output voltage magnitude can sometimes be much higher than the suitable voltage value required for battery charging purpose. Buck converter can be used as a voltage regulator, with the advantage of increasing the generated output current of the solar panel, while reducing its output voltage.
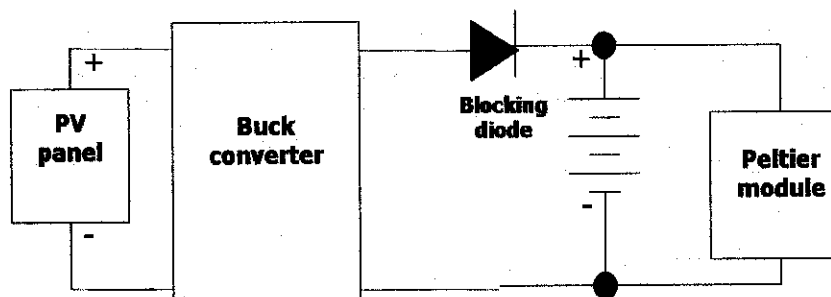
Figure 16   Power supply system design using Buck converter

Based on findings from the solar panel analysis, the average output voltage and current produced by the solar panel were estimated at 8.4V and 110mA. Using these values, the buck converter were designed.

For the buck converter design, a pulse width modulator (PWM) is required to produce square wave signals for switching purpose of the schematic. LM3524D chip has been acquired to perform this function. To design a buck converter, the LM3524D PWM chip's datasheet, by National Semiconductor is referred to. Please refer to **APPENDIX D** for the datasheet. **Figure 17** below is the schematic of the Buck converter as per the LM3524's datasheet.
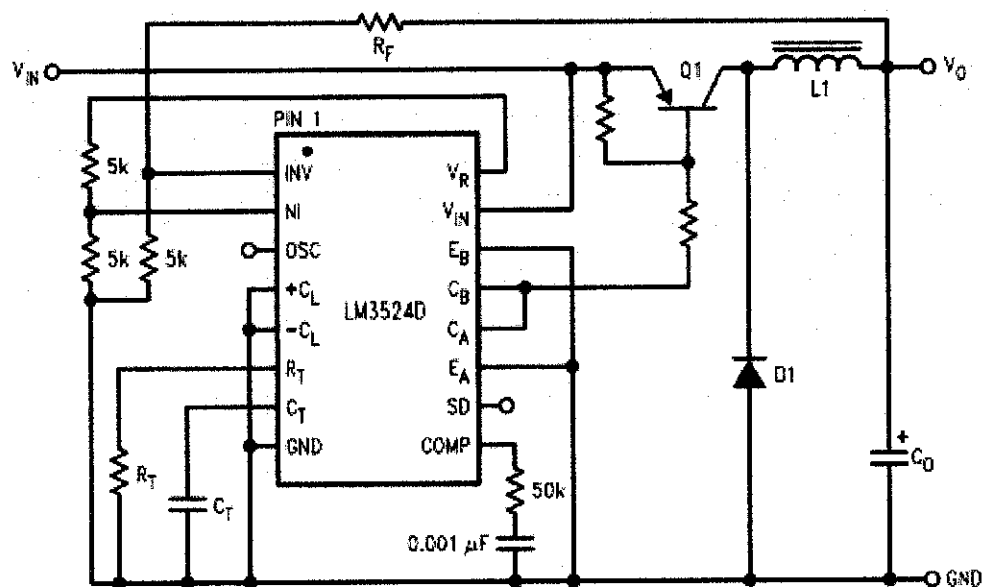
Figure 17   Buck converter schematic using LM3524D PWM[12]

To achieve output voltage and current values as desired, several components' values need to be calculated, namely R_F, R_T, C_T, C_O and L_1. Please refer to **APPENDIX C** for the calculation of the components. From calculation, the components values are:

1. $R_F = 10$ kΩ
2. $R_T = 300$ Ω
3. $C_T = 0.01 \mu F$
4. $C_O = 0.5$ μF
5. $L_1 = 49$ μH

For C_O and L_1, since it was difficult to find capacitor and inductor of exact values, the components were replace by a 0.47 µF capacitor and a 47 µH inductor, respectively.

From the datasheet the absolute maximum output current for each LM3524D is rated at 200mA. Operating the chip exceeding this limit could impose damage to it. Knowing that the maximum output current of the solar panel is 180mA, the designed buck converter might produce output current beyond this limit. Therefore for safe precaution, using components with calculated values, and the maximum solar panel outputs as the Buck converter input, the buck converter circuit was simulated using PSpice version 9.2.3 application tool. From the output simulation shown in **Figure 18**, it was observed that the resulting output current was 200mA, with a spike current signal that last less than 20 µs.
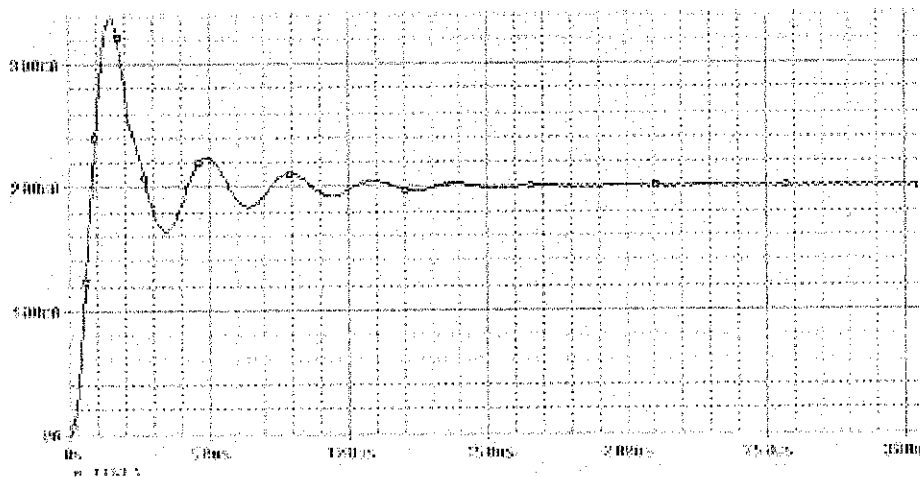
Figure 18   Buck converter simulation output using PSpice

As the simulated output for maximum input current indicates that the 200mA limit was not exceeded, design of the buck converter was proceeded on a breadboard, and to cater for output power from two solar panels, two buck converters were designed. When tested with the solar panel, the following outputs of the buck converters, which are tabulated in **Table 6** and **Table 7** were recorded.

Table 6   Tested output measurement of buck converter 1

Solar panel's output		Buck converter's output	
Voltage(V)	Current(mA)	Voltage(V)	Current(mA)
9.38	174	8.31	9.49
8.36	99	7.32	8.49
7.72	43	6.56	4.32

Table 7   Tested output measurement of buck converter 2

Solar panel's output		Buck converter's output	
Voltage(V)	Current(mA)	Voltage(V)	Current(mA)
9.4	176	8.68	10.31
8.4	123	7.74	8.68
7.7	49	6.99	5.27

From the results tabulated above, the output voltages of the Buck converters were as expected. Nevertheless, the output currents were much lower than expected. To overcome this, Darlington pair configuration is employed to boost up the Buck converter's output current. With this configuration, two transistors will be used instead of one previously.
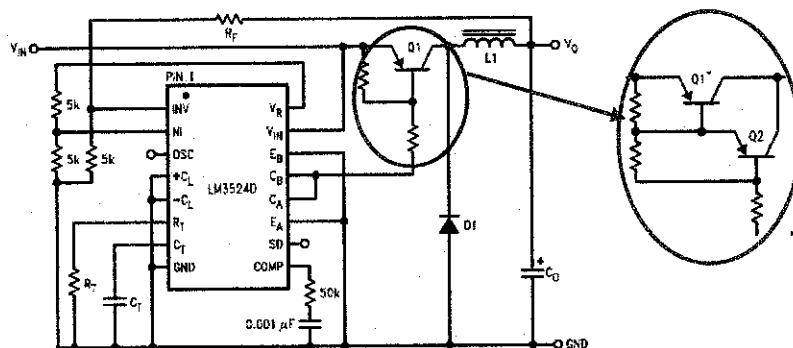
Figure 19   Implementation of Darlington pair transistors

After performing the modification, it was detected that only Buck converter 1 was functioning. **Table 8** below shows the recorded output measurement of Buck converter 1 after the modification.

Table 8   Tested output measurement of buck converter 1 using Darlington pair
          configuration

Solar panel's output		Buck converter's output	
Voltage(V)	Current(mA)	Voltage(V)	Current(mA)
9.22	143	8.47	82.54
8.28	116	7.45	64.31
7.71	51	6.83	34.45

4.2   Discussions

4.2.1   cooling load calculation

To calculate the heat load for a typical car cabin, Proton Wira Hatchback has been chosen as the case study. All calculations were based on the dimensions and structure of the car. The heat load calculated defined the cooling requirements for the temperature regulator system. The methods as well as the constant value used to calculate the heat load is acquired through the 2001 American Society of Heating, Refrigerating, and Air-Conditioning Engineers (ASHRAE) Fundamentals Handbook [13].

For the resulting calculated value of maximum cooling power needed for the design, all constant values obtained were taken for the worse case scenarios. The reason was to identify the highest possibility of heat load that may be presence in the vehicle cabin. In practical this value might be lower. One reason is that the vehicle doors and roof would have plastic cover, which will provide some thermal insulation. This would actually reduce the heat conducted by the doors and roof into the vehicle cabin. The load factor employ in the calculation represents the effect of humidity, with the value used is the maximum value for

a structure with close fitting doors, framing and windows. [13].

4.2.2 Peltier module and heatsink analysis

One of the objectives of conducting experiments on Peltier module and heatsink was to identify whether the heat dissipated by the Peltier module's hot side can be recycled to generate electricity. The main intention was to observe the possibility of reducing the dependency of solar panel for battery charging purpose.

From the results obtained, it was observed that the output current and voltage produced by Peltier module 2 were small. This was due to the fact that the temperature differences between the two Peltier module sides were not that very large. Even with the aid of improved heatsink, heat absorbed by the Peltier module 2's side which was in contact with the hot side of Peltier module 1 were still large enough, thus was able to increase the other Peltier module 2 side's temperature, which consequently contribute to the small temperature difference.
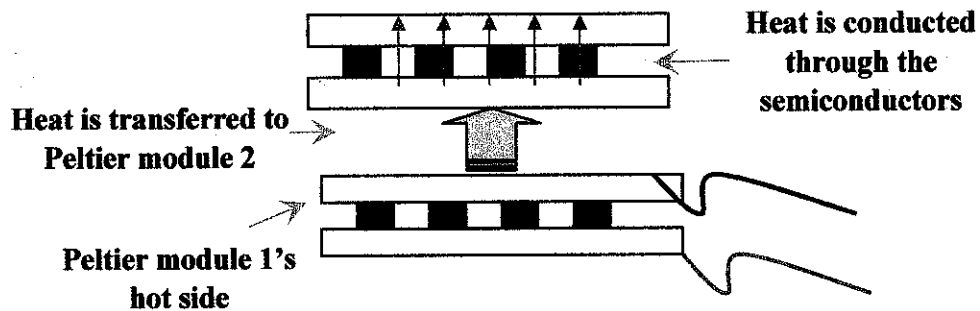
Figure 20   Heat transfer between the two Peltier modules

As the power generated by Peltier module is directly proportional to the temperature difference between the two sides, the smaller the differences would result in smaller generated power. It was concluded that recycling heat to harness electricity for the power supply system design, may not be practical for the design since the generated output were significantly small compared to the battery charging requirement.

4.2.3   Power supply system design

In designing the Buck converter, a Pulse Width Modulator (PWM) is required for switching purpose. An LM3524D PWM chip was acquired, and the configuration as per the datasheet was designed and implemented on a breadboard. However, from experimented test, the output current of the Buck converter was very small. Instead of becoming higher than the Buck converter input current, the resulting output current were extremely lower than the input current.

Darlington pair configuration was employed to boost up the output current. In this configuration, two transistors are connected together so that the amplified current from the first is amplified further by the second transistor.
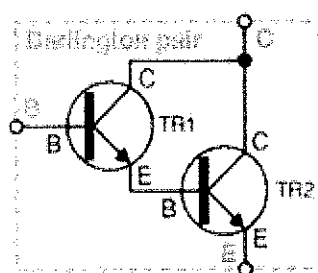
Figure 21   Darlington pair configuration

It was observed that output current increased after implementing the Darlington pair configuration, yet the magnitude was still smaller than the converter's input current. One possible reason for this outcome was that transistor Q1 and Q2 as well as the resistors connected to it as shown in **Figure 19** were not specified on their type or value. Thus, the resistors and transistors used in the real circuit might not be of the most suitable one. It was noted that the output current and voltages of the Buck converter varies with different values of resistors tested. In addition, losses that take place in the circuit, especially by the switching components, namely inductor and capacitor, contributed to the low output current. From this results, converter circuit was shown to experience losses. The use of it in the power supply system design would reduce the efficiency of the system.

As the temperature regulator design was planned for a small scale application, the power rating required, the dimension of solar panel, and heat sink may not

be much of a consideration. Furthermore the design was intended for demonstrating the power sourcing capability of the of the system for Peltier module only. When it comes to real application to a vehicle, the design may present certain setbacks. One of the with the problem is that it introduces battery in the system. To support the high power rating of the Peltier module, batteries with high power rating are needed. Batteries with such rating are usually big in sizes. Thus it may require some space to place them in the vehicle. It is proposed to place the batteries in the vehicle's luggage compartment or under the seats.

Suggested locations for batteries placement
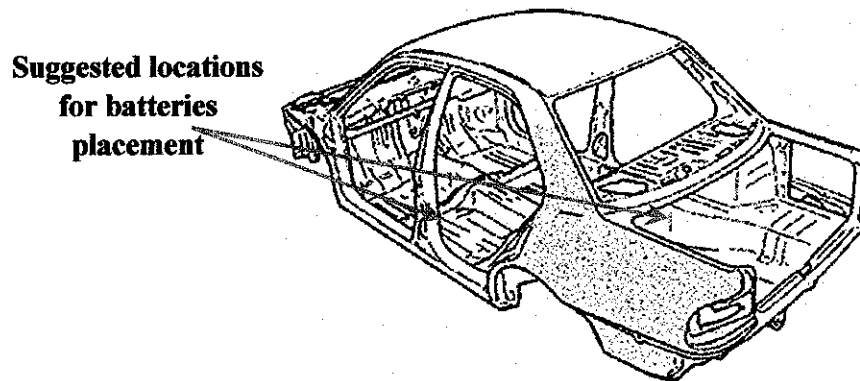
Figure 22   Suggested locations for battery placement

From the recorded vehicle cabin temperature, it can be generally predicted that for vehicle parked under sun-exposed condition, the Peltier module would have to be operational for a prolonged period of time. Suppose a user parked his or her vehicle at 8.00 in the morning, and leave it until 5.00 in the evening, assuming temperature of car cabin surpassed the triggering temperature threshold of 37°C at 10 a.m. This could render the Peltier module to operate up to 7 hours and perhaps more on a hot sunny day. Knowing that Peltier module draws very high current to function, and the expected cooling load as per calculation is incredibly large, batteries used in the system may likely to be drained quickly.

To prevent the likeliness of such occurrence, a battery with a high rating is therefore required. From findings, One of the highest Peltier module rating is a 267Watt module, From Hebeiltd Co. Ltd. [14]. Its maximum current and voltage ratings are 30.7A and 16.2V respectively. Assuming losses-free and 100% efficiency conversion of electricity to cooling power, eight of this rated

Peltier module can be connected in parallel to achieve a maximum 2136Watt of cooling power. This parallel connection would be capable to cater the 2006.32Watt maximum cooling power calculated. A 12V -1000Ah battery can be used as the power source.
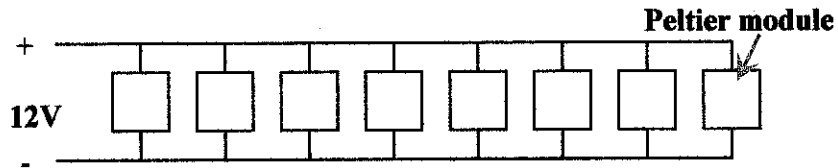
Figure 23   Parallel connection of Peltier module

Taking the maximum heat load as the targeted cooling capacity required, and each Peltier module operating at 12V, the current that each module would draw is 20.9 A. That will sum up to 167.2A. A battery current-rated at 1000Ah indicates that it can continuously provide 1000A of current for a period of one hour. For a load drawing 167.2A, the 1000Ah battery could supply current for about 6 long-hours.

The difficult part, however is in charging back the battery. Battery charger should have voltage rating higher than the battery. For a 12V battery, it is a common practice to use 14V battery charger. Usually for a long lasting battery maintenance, a battery is charged at one-tenth (0.1) of its 'Ah' rating for a period of 12 hours. This already indicates that the 1000Ah battery require twice the time of charging compare to the time it is powering the Peltier module. However, fast-charging can be allowed without being too frequent. It is important to highlight that for a 1000Ah battery, the solar panel may need to provide as much as 100A of charging current for a period of 12 hours.

Suppose, we can allow the battery to be charged at 0.2 of its 'Ah' rating, to have a charging time of 6 hours, which is the same amount of time it is discharging. The solar panel would therefore need to supply up to 200A. A solar panel of this capacity should be rated at (14V x 200A) or 2800Watt.

Solar panels are usually priced per watt of output power [16]. Surveys show that the cheapest available solar panel in the market is US$4.05/watt [17]. That would make up a total price of US$11,340 = RM43,092 for a 2800Watt solar panel. In addition, the space needed to allocate this power rated solar panel is

tremendously impractical. A 65.6Watt solar panel would already acquire a space of (0.94m X 0.5m)[7]. Another issue is that cloudy weather could reduce the output current of the solar panel. Just a slight variation of sun light intensity can influence the current that can be supplied by the solar panel, therefore increasing the amount of time to charge the battery.

The issues raised above is considering that the amount of cooling power need to be provided is the maximum calculated cooling power. However, suppose the vehicle cabin's temperature is at only 40°C, the required cooling power has already reach 1285.3Watt, which is still very large. The analysis above could provide a reliable deduction for the feasibility of using solar powered thermoelectric module to regulate vehicle cabin temperature.

CHAPTER 5

CONCLUSIONS AND RECOMMENDATIONS

5.1 Conclusions

Thermoelectric device provide a potential mean of cooling approaches. This is shown by the increasing number and variety of products which use thermoelectric technology [2]. Nevertheless, for a large scale application, this technology may not yet be feasible with present technology, as it draws very high current for operation. The use of Buck converter in the power supply system may introduce losses, which is not desired. Using solar panel as the sole power source for thermoelectric device may not be a practical approach, if the cooling load requirement is high. Nevertheless alternative power source can be exploited to aid the solar panel as a backup power source.

5.2 Recommendations

The Peltier module has the capability of removing heat from a medium, for which in this case, the air inside the vehicle cabin. To make use of this capability, the thermoelectric technology could be used together with vehicle having tinted windows. From the heat load calculation steps, it is obvious that glass windows are the major mean of which heat is transferred into the vehicle cabin. Tinted windows could filter out up to 80%[18] of this solar heat. Having lower heat load presence in the vehicle cabin, the Peltier module could function at much lower cooling power, hence lower, affordable power source.

One of the main concerns in using Peltier module for the project is the inability of solar panel of the appropriate size to charge the battery at a better rate than the rate the battery is being discharged. Faster charging rate would ensure that the batteries to be used in the system could provide the 'always-ready' power source desired. It is

41

recommended that charging circuitry is to be able to tap generated output power of the vehicle's alternator, when the engine is running. This could improve the time taken to charge a battery, hence reducing the solar panel dependency.

A better cooling mechanism, that can be used to cool the hot side of the module can be researched upon. As earlier stated, the better the cooling mechanism capability to remove heat from the module's hot side, the better the chances of only small heat conductivity from the module's hot side to the cold side. This could therefore increase temperature difference between the two sides, hence increasing the performance, as well as reducing the current drawn. In addition, if this is achieved, only then the Peltier module power generation capability can be considered as viable. This is because the greater the temperature difference between the two sides, the greater output power that will be generated.

REFERENCES

[1] Robert, 14 August 2004 http://www.vcontech.com/main.html

[2] Tellurex Corporation http://www.tellurex.com/12most.html

[3] Dallas Semiconductor, 1 December 2000 http://www.maxim.ic.com/support/

[4] http://www.thermoelectrics.com/introduction.htm

[5] Dane Lenaker, 4 April 2003 http://ffden_2.phys.uaf.edu/212

[6] Tellurex Corporation http://www.tellurex.com/TellurexPeltierFAQ.pdf

[7] July 1998, RS Data Sheet- solar panel.

[8] The British Photovoltaic Association

http://www.greenenergy.org.uk/pvuk2/technology/whatispv.html

[9] The British Photovoltaic Association

http://www.greenenergy.org.uk/pvuk2/technology/types.html

[10] 7 June 2004 http://www.xtremesystem.org/forums/showthread.php?t=38367

[11] Issa Batarseh, 2004, *Power Electronic Circuits*, : 136-138, John Wiley & Sons,

Inc.

43

[12] National Semiconductor, March 2005, LM2524D/LM3524D Regulating Pulse Width Modulator datasheet.

[13] 2001 American Society of Heating, Refrigerating, and Air-Conditioning Engineers (ASHRAE) Fundamentals Handbook (SI) (p. 28.4)

[14] Hebeiltd Co. Ltd., 28 August 2005,

http://www.hebeiltd.com.cn/?p=peltier.module

[15] J. Hewes, 2005, http://www.kpsec.freeuk.com/components/tran.htm

[16] 16 March 2005, http://www.otherpower.com/otherpower_solar.html

[17] 10 October 2005,

http://www.ecobusinesslinks.com/solar_panels_cheap_used_supply.htm

[18] Bengt Halvorson, 6 November 2005,

http://www.thecarconnection.com/Enthusiasts/Maintenance_Tips/s277.html

APPENDICES

Appendix A : HEAT LOAD CALCULATION

Appendix B : PROTON WIRA HATCHBACK'S DIMENSIONS

Appendix C : BUCK CONVERTER'S COMPONENTS CALCULATION

Appendix D : LM3524D DATASHEET

Appendix E : PICTURES GALLERY

APPENDIX A

HEAT LOAD CALCULATION

The cooling loads caused by **conduction** heat gains through the roof and doors are found from the following equation:

$$Q = U \times A \times CLTD$$

Where

Q   = cooling load for roof, or the doors (W)

U   = overall heat transfer coefficient for roof or the doors (W/(m²K))

A   = area of roof (m²)

CLTD = corrected cooling load temperature difference (K)

> *The CLTD is a modified value of the temperature difference between the outdoor and indoor air that accounts for heat storage and exposure effect of the sun.*
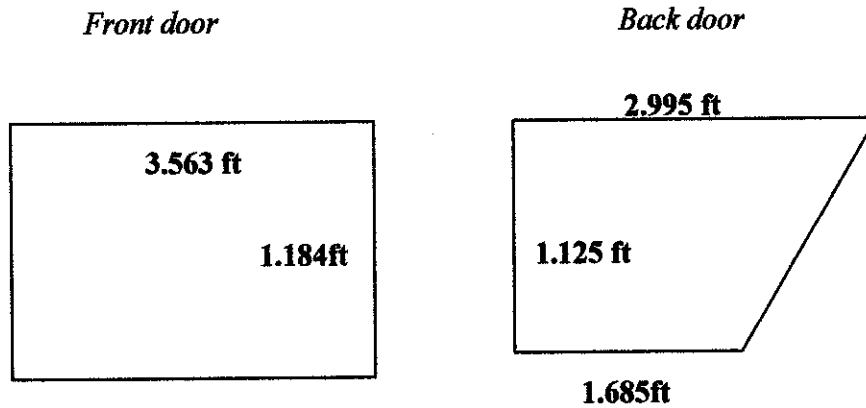
Roof load calculation

(Please refer to **APPENDIX B** for reference of dimension)

4.816 ft

3.215 ft
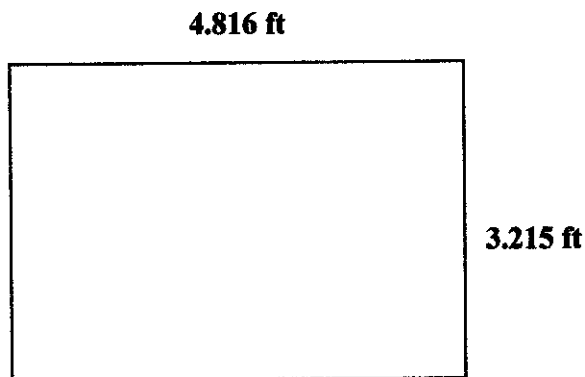
$Q_1 = U \times A \times CLTD$

$= (1.21)(15.483 \text{ ft}^2)(24.3)$

$= (1.21)(1.43992 \text{ m}^2)(24.3)$

$= 42.337 \ W$

<u>Door load calculation</u>

(Please refer to **APPENDIX B** for reference of dimension)

Front door   *Back door*

2.995 ft

3.563 ft

1.184ft   **1.125 ft**

1.685ft

$Q_2 = U \times A \times CLTD \times 2[\text{for both sides}]$

$= (1.21)(6.8521 \text{ ft}^2)(11.3)(2)$

$= (1.21)(0.6373 \text{ m}^2)(11.3)(2)$

$= 17.428 \ W$

Radiant energy from the sun passes through transparent materials such as glass windows can become a source of heat gain to the vehicle cabin. Its values varies with time, orientation, shading and storage effect. The **radiation** load can be found from the following equation:
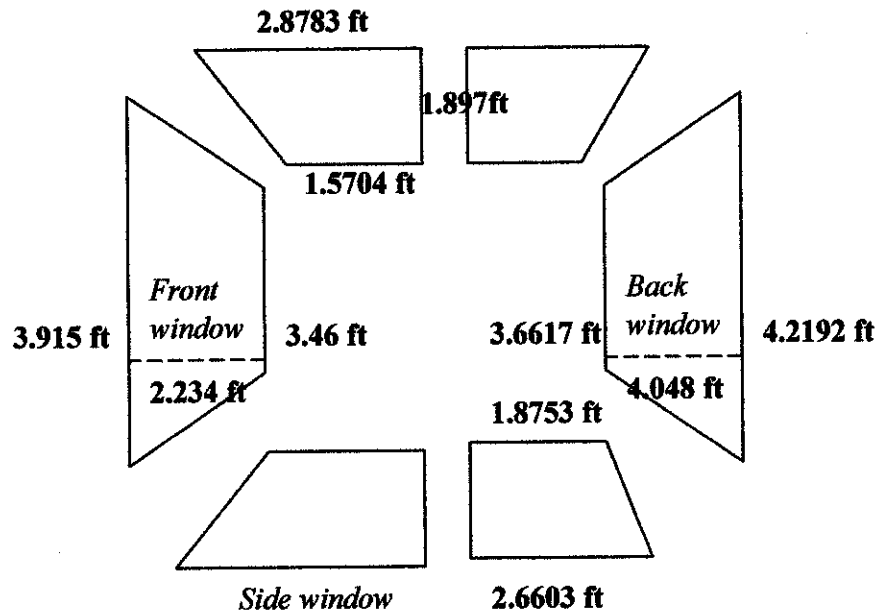
$$Q = (GLF)A$$

Where jump

Q   = cooling load for glass and windows (W)

A   = area of glass (m^2)

GLF   = glass load factor, which include the effects of both soar transmission and

radiation (K)

Glass load calculation

(Please refer to **APPENDIX B** for reference of dimension)

$$Q_3 = (GLF)A$$

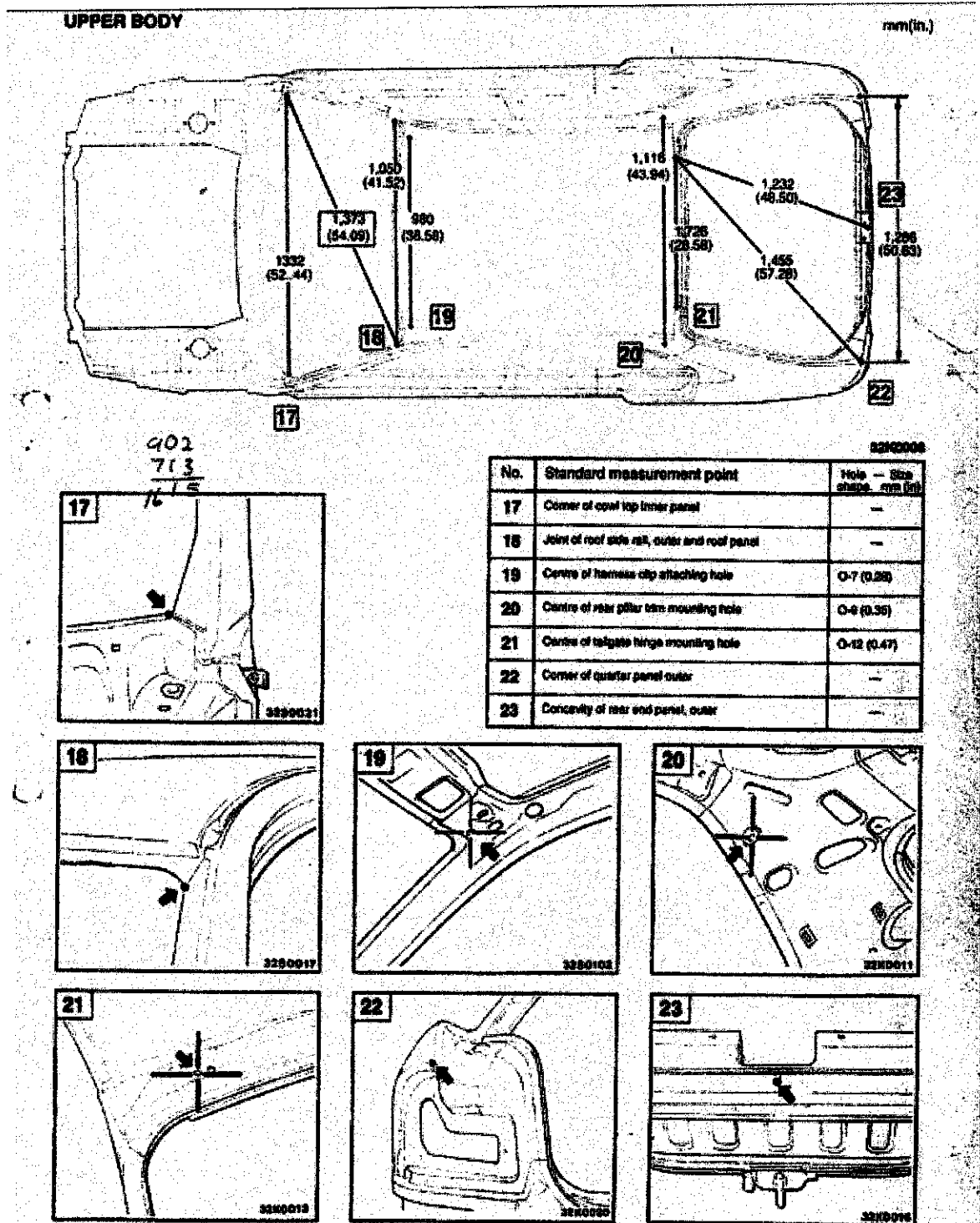$$= (2.2968)(290.9) + (0.8257)(120.5) + (0.8257)(179.43)$$

$$= 915.79\ W$$

Total load = Total heat load x Load Factor

$$= (Q1 + Q2 + Q3) \times (1.24)$$

$$= (42.337W + 17.428\ W + 915.79\ W) = \mathbf{1209.69\ W}$$

UPPER BODY — mm(in.)

No.	Standard measurement point	Hole — Size shape, mm (in)
17	Corner of cowl top inner panel	—
18	Joint of roof side rail, outer and roof panel	—
19	Centre of harness clip attaching hole	O-7 (0.28)
20	Centre of rear pillar trim mounting hole	O-9 (0.35)
21	Centre of tailgate hinge mounting hole	O-12 (0.47)
22	Corner of quarter panel outer	—
23	Concavity of rear end panel, outer	—

Dimensions shown in diagram:
- 1,050 (41.52)
- 1,373 (54.09)
- 980 (38.58)
- 1332 (52.44)
- 1,116 (43.94)
- 1,232 (48.50)
- 1,726 (28.58)
- 1,296 (50.63)
- 1,455 (57.28)

mm(in.)

32K0010

32K0009

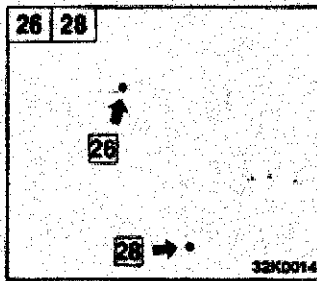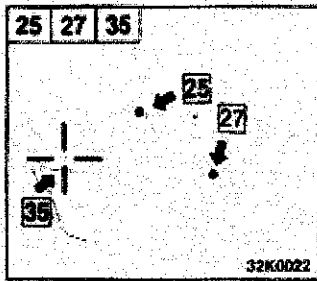| No.	Standard measurement point	Hole — Size shape, mm (in)	No.	Standard measurement point	Hole — Size shape, mm (in)
24	Front pillar positioning notch (Upper section)	—	32	Rear pillar positioning notch (Upper section)	—
25	Front pillar positioning notch (Lower section)	—	33	Rear pillar positioning notch (lower section)	—
26	Joint of roof side rail outer and center pillar, outer	—	34	Centre of front door hinge mounting hole (Upper section)	O-10 (0.39)
27	Joint of front pillar outer and side sill outer	—	35	Centre of front door hinge mounting hole (Lower section)	O-10 (0.39)
28	Center pillar positioning notch (Upper section)	—	36	Centre of rear door hinge mounting hole (Upper section)	O-10 (0.39)
29	Center pillar positioning notch (Lower section)	—	37	Centre of rear door hinge mounting hole (Lower section)	O-10 (0.39)
30	Joint of roof side rail outer and quarter panel, outer	—	38	Centre of rear door switch mounting hole	O-5 (0.20)
31	Joint of center pillar outer and side sill outer	—			

32K0022

32K0014

32K0012
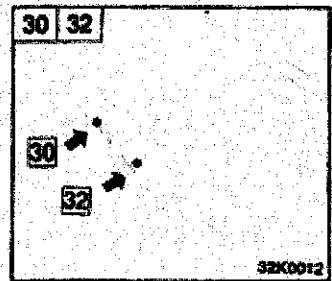
UNDER BODY

No.	Standard measurement point	Hole — Size shape, mm (in)	No.	Standard measurement point	Hole — Size shape, mm (in)
1*	Centre of front bumper mounting hole	O-13 (0.51)	5*	Rear portion of rear seat crossmember positioning hole	O-68x68 (2.67 x 1.80)
2	Rear portion of front sidemember positioning hole	O-25 (0.98)	6	Centre of rear floor sidemember drain hole	O-20 (0.79)
3*	Centre of suspension crossmember mounting hole	O-16 (0.63)	7*	Rear portion of rear floor sidemember extension positioning hole	O-40 x 70 (0.79 x 2.76)
4*	Rear portion of front floor sidemember positioning hole	O-25 (0.98)			

NOTE: the * mark indicates the mounting position for the frame centering gauge.
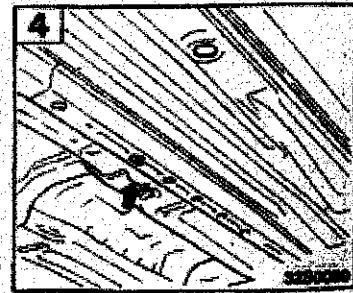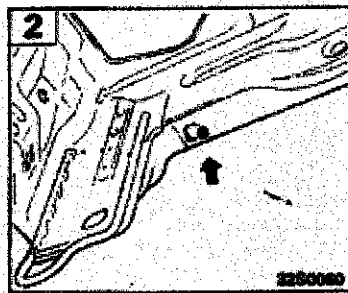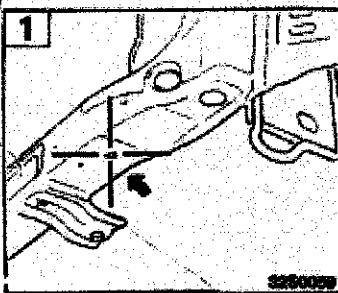
APPENDIX C

BUCK CONVERTER'S COMPONENTS CALCULATION

Please refer to **APPENDIX D** for reference of formulas acquired to calculate the components.

Below is the predetermined values of the Buck converter:

1. $V_O = 7.5V$
2. $= 8.4V$
3. $I_{in} = 110mA$
4. $f = 333kHz$
5. output ripple voltage = 0.5% ($\Delta V_O/V_O = 0.005$)

Value of $I_O = (V_{in} / V_O)I_{in}$

$\qquad = (8.4V/7.5V)(110 \text{ mA})$

$\qquad = 123 \text{ mA}$

Value of $R_F = 5k\Omega ([V_O /2.5] - 1)$

$\qquad = 5k\Omega ([7.5 /2.5] - 1)$

$\qquad = \textbf{10 k}\boldsymbol{\Omega}$

It was determined to select value of $R_T = \textbf{300 } \boldsymbol{\Omega}$

Value of $C_T = 1/(f)(R_T)$

$\qquad = 1/(333kHz)(300 \ \Omega)$

$\qquad = \textbf{0.01 } \boldsymbol{\mu F}$

Value of $L_1 = (2.5[V_{in} - V_O] V_O) \div ([I_O][f][V_{in}])$

$\qquad = (2.5[0.9] 7.5) \div ([0.123][333 \times 10^{-3}][8.4])$

$\qquad = \textbf{49 } \boldsymbol{\mu H}$

Value of $C_O = ([V_{in} - V_O] T^2 V_O) \div (8\Delta V_O V_{in} L_1)$

$\qquad = ([8.4-7.5][3 \times 10^{-6}]^2)(200) \div (8 [7.5][49 \ \mu H])$

$\qquad = \textbf{0.5 } \boldsymbol{\mu F}$

APPENDIX D

LM3524D DATASHEET

Absolute Maximum Ratings (Note 5)

If Military/Aerospace specified devices are required, please contact the National Semiconductor Sales Office/ Distributors for availability and specifications.

Supply Voltage	40V
Collector Supply Voltage	
(LM2524D)	55V
(LM3524D)	40V
Output Current DC (each)	200 mA
Oscillator Charging Current (Pin 7)	5 mA

Internal Power Dissipation	1W
Operating Junction Temperature	
Range (Note 2)	
LM2524D	−40°C to +125°C
LM3524D	0°C to +125°C
Maximum Junction Temperature	150°
Storage Temperature Range	−65°C to +150°C
Lead Temperature (Soldering 4 sec.)	
M, N Pkg.	260°C

Electrical Characteristics
(Note 1)

Symbol	Parameter	Conditions	LM2524D			LM3524D			Units
			Typ	Tested Limit (Note 3)	Design Limit (Note 4)	Typ	Tested Limit (Note 3)	Design Limit (Note 4)	
REFERENCE SECTION									
V_{REF}	Output Voltage		5	4.85	4.80	5	4.75		V_{Min}
				5.15	5.20		5.25		V_{Max}
V_{RLine}	Line Regulation	V_{IN} = 8V to 40V	10	15	30	10	25	50	mV_{Max}
V_{RLoad}	Load Regulation	I_L = 0 mA to 20 mA	10	15	25	10	25	50	mV_{Max}
$\frac{\Delta V_{IN}}{\Delta V_{REF}}$	Ripple Rejection	f = 120 Hz	66			66			dB
I_{OS}	Short Circuit Current	V_{REF} = 0	50	25		50	25		mA Min
				180			200		mA Max
N_O	Output Noise	10 Hz ≤ f ≤ 10 kHz	40		100	40		100	$\mu V_{rms\ Max}$
	Long Term Stability	T_A = 125°C	20			20			mV/kHr
OSCILLATOR SECTION									
f_{OSC}	Max. Freq.	R_T = 1k, C_T = 0.001 µF (Note 7)	550		500	350			kHz_{Min}
f_{OSC}	Initial Accuracy	R_T = 5.6k, C_T = 0.01 µF (Note 7)	20	17.5		20	17.5		kHz_{Min}
				22.5			22.5		kHz_{Max}
		R_T = 2.7k, C_T = 0.01 µF (Note 7)	38	34		38	30		kHz_{Min}
				42			46		kHz_{Max}
Δf_{OSC}	Freq. Change with V_{IN}	V_{IN} = 8 to 40V	0.5	1		0.5	1.0		$\%_{Max}$
Δf_{OSC}	Freq. Change with Temp.	T_A = −55°C to +125°C at 20 kHz R_T = 5.6k, C_T = 0.01 µF	5			5			%
V_{OSC}	Output Amplitude (Pin 3) (Note 8)	R_T = 5.6k, C_T = 0.01 µF	3	2.4		3	2.4		V_{Min}
t_{PW}	Output Pulse Width (Pin 3)	R_T = 5.6k, C_T = 0.01 µF	0.5	1.5		0.5	1.5		μs_{Max}
	Sawtooth Peak Voltage	R_T = 5.6k, C_T = 0.01 µF	3.4	3.6	3.8		3.8		V_{Max}

Electrical Characteristics (Continued)
(Note 1)

Symbol	Parameter	Conditions	LM2524D			LM3524D			Units
			Typ	Tested Limit (Note 3)	Design Limit (Note 4)	Typ	Tested Limit (Note 3)	Design Limit (Note 4)	
TC-V$_{sense}$	Sense Voltage T.C.		0.2			0.2			mV/°C
	Common Mode Voltage Range	V$_6$ – V$_4$ = 300 mV	-0.7 1			-0.7 1			V$_{Min}$ V$_{Max}$
SHUT DOWN SECTION									
V$_{SD}$	High Input Voltage	V$_{(Pin\ 2)}$ – V$_{(Pin\ 1)}$ ≥ 150 mV	1	0.5 1.5		1	0.5 1.5		V$_{Min}$ V$_{Max}$
I$_{SD}$	High Input Current	I$_{(pin\ 10)}$	1			1			mA
OUTPUT SECTION (EACH OUTPUT)									
V$_{CES}$	Collector Emitter Voltage Breakdown	I$_C$ ≤ 100 µA		55			40		V$_{Min}$
I$_{CES}$	Collector Leakage Current	V$_{CE}$ = 60V							µA$_{Max}$
		V$_{CE}$ = 55V	0.1	50					
		V$_{CE}$ = 40V				0.1	50		
V$_{CESAT}$	Saturation Voltage	I$_E$ = 20 mA	0.2	0.5		0.2	0.7		V$_{Max}$
		I$_E$ = 200 mA	1.5	2.2		1.5	2.5		
V$_{EO}$	Emitter Output Voltage	I$_E$ = 50 mA	18	17		18	17		V$_{Min}$
t$_R$	Rise Time	V$_{IN}$ = 20V, I$_E$ = –250 µA, R$_C$ = 2k	200			200			ns
t$_F$	Fall Time	R$_C$ = 2k	100			100			ns
SUPPLY CHARACTERISTICS SECTION									
V$_{IN}$	Input Voltage Range	After Turn-on		8 40			8 40		V$_{Min}$ V$_{Max}$
T	Thermal Shutdown Temp.	(Note 2)	160			160			°C
I$_{IN}$	Stand By Current	V$_{IN}$ = 40V (Note 6)	5	10		5	10		mA

Note 1: Unless otherwise stated, these specifications apply for T$_A$ = T$_J$ = 25°C. Boldface numbers apply over the rated temperature range: LM2524D is –40° to 85°C and LM3524D is 0°C to 70°C. V$_{IN}$ = 20V and f$_{OSC}$ = 20 kHz.

Note 2: For operation at elevated temperatures, devices in the N package must be derated based on a thermal resistance of 86°C/W, junction to ambient. Devices in the M package must be derated at 125°C/W, junction to ambient.

Note 3: Tested limits are guaranteed and 100% tested in production.

Note 4: Design limits are guaranteed (but not 100% production tested) over the indicated temperature and supply voltage range. These limits are not used to calculate outgoing quality level.

Note 5: Absolute maximum ratings indicate limits beyond which damage to the device may occur. DC and AC electrical specifications do not apply when operating the device beyond its rated operating conditions.

Note 6: Pins 1, 4, 7, 8, 11, and 14 are grounded; Pin 2 = 2V. All other inputs and outputs open.

Note 7: The value of a C$_t$ capacitor can vary with frequency. Careful selection of this capacitor must be made for high frequency operation. Polystyrene was used in this test. NPO ceramic or polypropylene can also be used.

Note 8: OSC amplitude is measured open circuit. Available current is limited to 1 mA so care must be exercised to limit capacitive loading of fast pulses.

Typical Applications (Continued)

Design Equations

$$R_2 = 5\,k\Omega \left(\frac{V_0}{2.5} - 1\right)$$
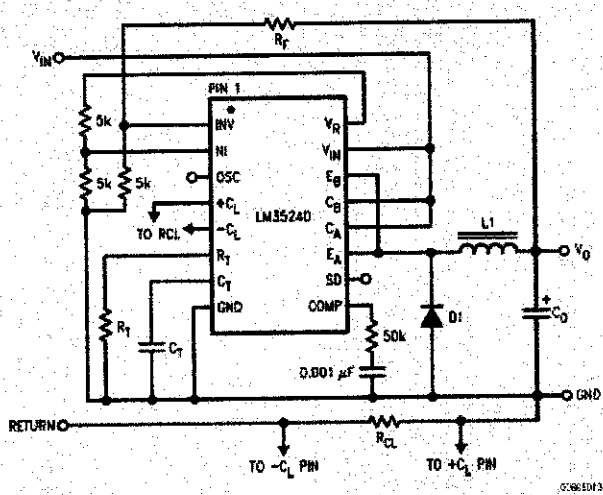
$$R_{CL} = \frac{\text{Current Limit Sense Volt}}{I_{o(MAX)}}$$

$$f_{OSC} = \frac{1}{R_T C_T}$$

$$L1 = \frac{2.5 V_0 (V_{IN} - V_0)}{I_0 V_{IN} f_{OSC}}$$

$$C_0 = \frac{(V_{IN} - V_0) V_0 T^2}{8 \Delta V_0 V_{IN} L1}$$

$$I_{o(MAX)} = I_{IN} \frac{V_{IN}}{V_0}$$

FIGURE 9. Positive Regulator. Step-Down Basic Configuration ($I_{IN(MAX)} = 80$ mA)

56
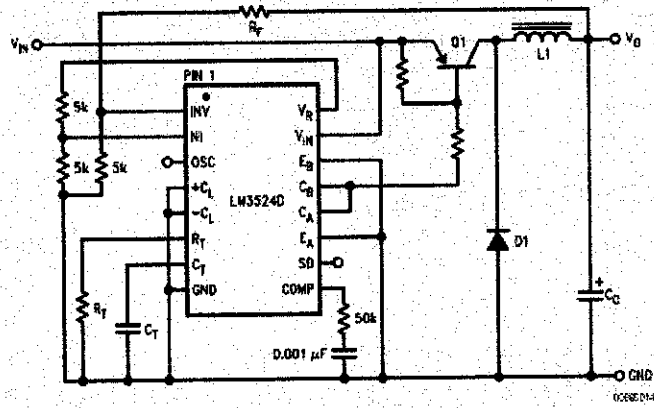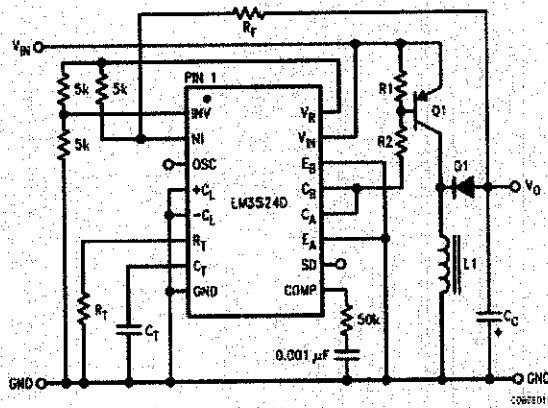
Typical Applications (Continued)

FIGURE 10. Positive Regulator, Step-Down Boosted Current Configuration

Design Equations

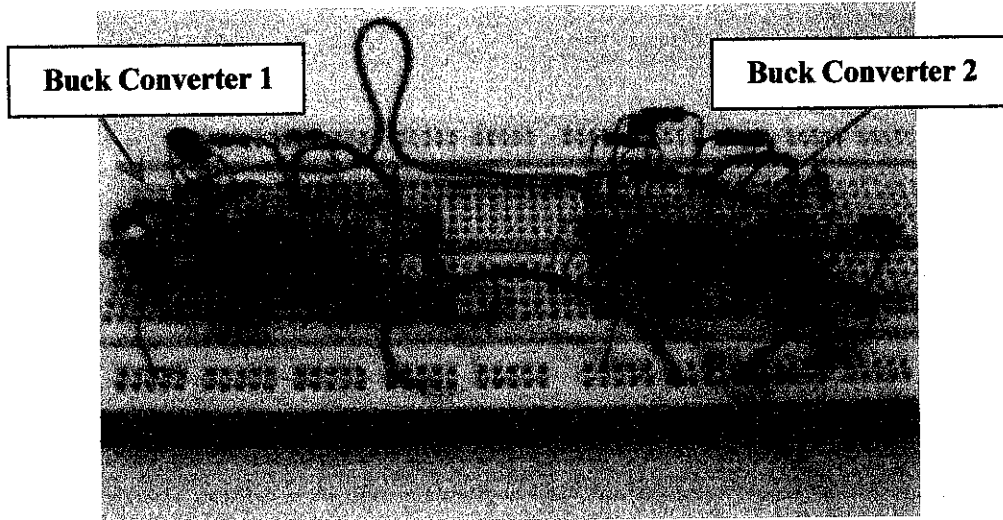$$R_F = 5k \left(1 - \frac{V_C}{2.5} \right)$$

$$f_{OSC} = \frac{1}{R_T C_T}$$

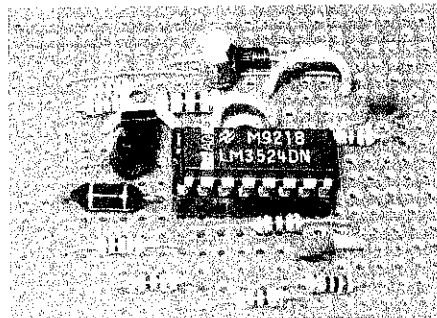$$L1 = \frac{2.5 V_{IN} V_O}{f_{OSC} (V_O + V_{IN}) I_O}$$

$$C_O = \frac{I_O V_O}{\Delta V_O f_{OSC} (V_O + V_{IN})}$$

FIGURE 11. Boosted Current Polarity Inverter

57

APPENDIX E
PICTURE GALLERY

Buck converter design implementation on breadboard

Buck converter design on veraboard using Darlington transistors configuration

Peltier module and heatsink analysis

Peltier module with improved heatsink analysis